

Laboratory arrangement for soft x-ray zone plate efficiency measurements

Michael C. Bertilson, Per A. C. Takman, Anders Holmberg,

Ulrich Vogt, and Hans M. Hertz

Biomedical and X-Ray Physics, Department of Applied Physics, Royal Institute of Technology, AlbaNova, SE-106 91 Stockholm, Sweden

(Received 21 November 2006; accepted 12 January 2007; published online 27 February 2007)

We demonstrate a laboratory-scale arrangement for rapid and accurate measurements of the absolute and local efficiency of soft x-ray micro zone plates in the water window. This in-house instrument is based on a single-line $\lambda=2.88$ nm liquid-jet laser-plasma source. Measurements are performed by a simultaneous comparison of first diffraction-order photon flux with the flux in a calibrated reference signal. This arrangement eliminates existing source emission fluctuations. The performance of the method is demonstrated by the result from measurements of two $\sim 55\text{ }\mu\text{m}$ diameter nickel micro zone plates, showing a groove efficiency of $12.9\%\pm 1.1\%$ and $11.7\%\pm 1.0\%$. Furthermore, we show that spatially resolved efficiency mapping is an effective tool for a detailed characterization of local zone plate properties. Thus, this laboratory-scale instrument allows rapid feedback to the fabrication process which is important for future improvements. © 2007 American Institute of Physics. [DOI: [10.1063/1.2472590](https://doi.org/10.1063/1.2472590)]

High-resolution soft x-ray microscopes exclusively use so-called micro zone plates (MZPs) as optics for the objective.^{1,2} These zone plates, which are circular diffraction gratings with a radially decreasing grating constant, are manufactured by modern nanolithography methods. To judge the quality of a zone plate the absolute efficiency, which is the ratio between the diffracted light in a certain order (normally first order) and the incoming radiation, is often used. In the present article we demonstrate an in-house method for measuring the local MZP efficiency using a compact liquid-jet-target laser-plasma source.

The complex index of refraction can be given as $n=1-\delta+i\beta$, where typical values for δ and β are in the range of $10^{-3}-10^{-6}$ for x-ray radiation. Therefore, refractive lenses cannot be used as optical elements, and instead diffractive zone plate optics are employed. In a water-window soft x-ray microscope operating, e.g., close to the oxygen *K* edge ($\lambda=2.4$ nm), zone plates can be used both for the condenser and the objective. While typical condenser diameters are in the range of millimeters, typical diameters for objectives are a few tens micrometers. The main issues for these micro zone plates are resolution and efficiency. Both parameters require specialized processing techniques suitable for deep periodic narrow-linewidth structures. For water-window soft x-rays, nickel is a common zone plate material. Our nickel zone plate fabrication method is based on a trilayer resist scheme, and the important process steps are electron-beam lithography for the basic pattern generation, reactive ion etching for the creation of a polymer mold, and nickel electroplating of the final optical element.³

The efficiency characterization of fabricated optics is very important for their later application in a microscope, since this will have a direct impact on the exposure times. Moreover, an efficiency measurement can give a direct feedback to the fabrication process with respect to, e.g., zone height and line-to-space ratio. So far, most such characterization measurements have been performed with synchrotron

radiation in combination with grating monochromators for wavelength selectivity.⁴⁻⁷

In the present article we present an in-house method for the absolute and local efficiency measurement of MZPs using a compact laser-plasma source. The use of a single plasma-emission line eliminates the need for a monochromator, and existing emission fluctuations are eliminated by the monitoring of reference signals. The laboratory-scale and in-house availability of the arrangement allows rapid feedback to the fabrication process which is important for future improvements.

Figure 1 shows a schematic illustration of the arrangement which consists of a soft x-ray liquid-nitrogen-jet laser-plasma source,⁸ spectral and damping filters, the MZP to be measured, two reference pinholes, an order-sorting aperture (OSA) and finally a soft x-ray sensitive charge coupled device (CCD). Since soft x rays are absorbed in air, the entire arrangement is operated in vacuum and all optical elements are positioned using computer-controlled translation stages.

The soft x-ray plasma source is created by focusing a pulsed, 100 Hz, ~ 3 ns, frequency-doubled Nd:YAG (yttrium aluminum garnet) laser (Coherent Infinity 40–100) with ~ 200 mJ pulses onto a $\sim 20\text{ }\mu\text{m}$ liquid-nitrogen jet resulting in a source size of $\sim 20\text{ }\mu\text{m}$ full width at half maximum. The emitted spectrum consists of a continuous low-intensity blackbody spectrum and two superimposed predominant emission lines, N VI ($\lambda=2.88$ nm) and N VII ($\lambda=2.48$ nm). The bandwidth of these emission lines is typically $\lambda/\Delta\lambda>500$ (Ref. 9), and the brightness is of the order of 10^8 photons/(pulse sr μm^2 line).⁸ A 600 nm titanium foil acts as a spectral filter, thereby providing efficient suppression of the $\lambda=2.48$ nm line while still having high transmission for the $\lambda=2.88$ nm line. The transmitted spectrum consists of a narrow peak at $\lambda=2.88$ nm, yielding a signal ~ 250 times stronger compared to the unwanted $\lambda=2.48$ nm peak, which is the main contribution from the remaining spectrum.

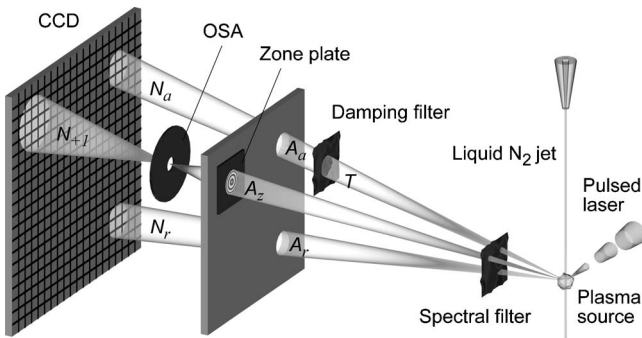


FIG. 1. A schematic illustration showing the main components of the experimental arrangement used for determining the efficiency and quality of micro zone plates.

The MZP to be measured is mounted at a distance of ~ 460 mm from the source and ~ 18 mm from the CCD chip, using a thin gel-like film (Gel-Film® by Gel-Pak) for easy removal. The investigated MZPs in this article have a diameter of $54.5\ \mu\text{m}$, ~ 550 zones, an outer zone width of $25\ \text{nm}$, a mean zone height of $\sim 140\ \text{nm}$, and a focal length of $\sim 470\ \mu\text{m}$ at $\lambda=2.88\ \text{nm}$. The MZP structure rests on a supporting membrane consisting of $5\ \text{nm}$ chromium, $10\ \text{nm}$ germanium, and $50\ \text{nm}$ silicon nitride (Si_3N_4), which has a transmission of $\sim 65\%$ at $\lambda=2.88\ \text{nm}$. MZPs diffract radiation into several orders, $m=\pm 1, 2, 3, \dots$, and in order to measure the first order efficiency, the other orders must be blocked. Higher orders, $|m|>1$, are blocked by a $\sim 5\ \mu\text{m}$ OSA placed in the first order image plane of the source. The small diameter of the OSA also reduces the zeroth order and limits its extension on the CCD to only a few pixels.

Two $\sim 600\ \mu\text{m}$ pinholes, placed beside the MZP, enable the monitoring of two reference signals. The large intensity ratio ($\sim 10^4$) between CCD pixels illuminated by the first order and pixels directly illuminated through a pinhole makes it impossible to accurately measure both signals within the dynamic range of the CCD. Accuracy is improved by the utilization of the second reference signal, which is attenuated by a $500\ \text{nm}$ titanium and a $400\ \text{nm}$ germanium foil with a measured transmission of $\sim 3.3\%$ at the present wavelength $\lambda=2.88\ \text{nm}$. The unattenuated reference signal can be blocked to protect the CCD during long exposures of weaker signals.

The photon detector is a back-side-illuminated, soft x-ray sensitive 16 bit CCD (ANDOR Technology) with 1024×1024 pixels and a pixel size of $13\times 13\ \mu\text{m}^2$.

It should be noted that the arrangement can easily be modified to perform efficiency measurements of either MZPs or condenser zone plates with larger diameters and longer focal lengths.

The zone plate efficiency measurements are based on indirect measurements of fluxes and can be derived from the definition of absolute zone plate efficiency,

$$\eta = \frac{\Phi_{+1}}{\Phi_z}, \quad (1)$$

where Φ_{+1} is the first diffraction-order photon flux of the MZP and Φ_z the total photon flux collected by the MZP. Φ_{+1} can be determined by the number of detected first order photons N_{+1} divided by the exposure time t , $\Phi_{+1}=N_{+1}/t$. In practice, it is not feasible to directly measure the incident photon

flux Φ_z . However, the high isotropy of the emitted radiation from the source within the small angular separation between the MZP and the reference pinhole, $\sim 17\ \text{mrad}$, makes it possible to indirectly measure it via the attenuated reference signal N_a ,

$$\Phi_z = \frac{N_a \cdot A_z}{T \cdot A_a \cdot t}, \quad (2)$$

where T is the transmission of the damping filter, A_z the area of the MZP, A_a the area of the attenuated reference pinhole and, t the exposure time (Fig. 1). The efficiency can now be determined by combining Eqs. (1) and (2),

$$\eta = \frac{N_{+1}}{N_a} \cdot \frac{A_a}{A_z} \cdot T. \quad (3)$$

Given the damping filter transmission and MZP and pinhole areas, the zone plate efficiency could be determined by simply measuring the ratio between detected photons in the MZP's first order and the attenuated reference signal, N_{+1}/N_a .

In reality the damping filter transmission is unknown, and therefore a complete efficiency measurement is performed in two steps. For clarity the measured quantities from each step are denoted with I and II. In a first (I) exposure the unknown damping filter transmission T is measured via

$$T = \frac{N_a^I}{N_r^I} \cdot \frac{A_r}{A_a}, \quad (4)$$

where N_a^I/N_r^I is the ratio between detected photons in the attenuated and unattenuated reference signal, and A_a and A_r are the corresponding reference pinhole areas. In the second exposure (II) the photon ratio N_{+1}^{II}/N_a^{II} is measured while blocking the unattenuated reference pinhole for CCD protection. The efficiency is finally determined by the combination of Eqs. (3) and (4),

$$\eta = \frac{N_{+1}^{II}}{N_a^{II}} \cdot \frac{N_a^I}{N_r^I} \cdot \frac{A_r}{A_z}, \quad (5)$$

which only contains the two measured photon ratios, the size of the MZP, and the size of the unattenuated reference pinhole. The effects of exposure time uncertainties and temporal source intensity fluctuations are eliminated because each photon ratio is determined in a single exposure.

We demonstrate the arrangement by presenting results obtained from measurements of two in-house fabricated MZPs (Ref. 3) (denoted A and B). The zone plate design parameters for these MZPs are identical except that zone plate A was exposed with a lower electron dose during the e-beam writing process compared to B. All aperture and zone plate dimensions were carefully measured using a scanning electron microscope and an interferometric table to minimize contributions to systematic errors. The final efficiency was determined from a series of ten measurements to reduce the impact of noise and statistical uncertainties. Each measurement was based on a $\sim 0.02\ \text{s}$ reference ray calibration exposure (I) and a $\sim 2\ \text{s}$ MZP exposure (II). The final results show an absolute efficiency of $\eta_A=8.4\%\pm 0.5\%$ for MZP A and $\eta_B=7.6\%\pm 0.5\%$ for MZP B. Given the $\sim 65\%$ transmission of the supporting silicon nitride (Si_3N_4) membrane, these total efficiencies correspond to a groove efficiency of $12.9\%\pm 1.1\%$ and $11.7\%\pm 1.0\%$, respectively. The esti-

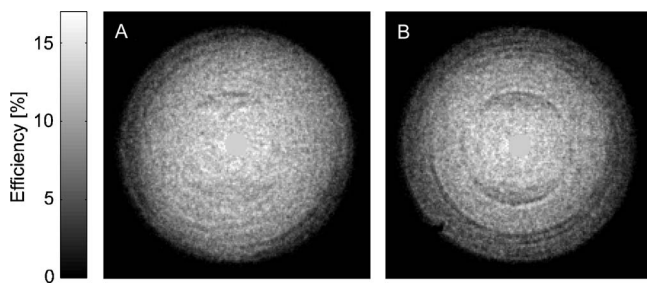


FIG. 2. Maps showing the local efficiency of zone plates A and B. Noise has been reduced in both maps by computing the average from ten measurements.

mated uncertainties correspond to two standard deviations and are based on statistical and systematic errors. The relative statistical error for one typical measurement is around $2\sigma/\eta \approx 3\%$ and the total relative systematic error is $\Delta\eta/\eta \approx 5\%$, yielding a total relative measurement error of $\sim 6\%$ when based on ten measurements per MZP. In the total systematic error we have considered the following error contributions: MZP area and reference pinhole area uncertainties, spectral filter transmission variations, detection of unwanted ($\lambda \neq 2.88$ nm) photons in the unattenuated reference signal, detector nonlinearities, and errors introduced during the analysis of experimental data. Previous efficiency measurements of MZPs have been performed on synchrotrons, which are known to suffer from problems with higher orders of unwanted wavelengths, resulting in larger errors compared to measurements performed with the method presented here.⁷

Figure 2 presents local efficiency maps of MZPs A and B. These maps are the computed average of the two measurement series and therefore noise is reduced by $\sim 70\%$, which makes local efficiency variations more prominent. The most central pixels are dominated by unwanted zero-order photons. In the efficiency maps presented in Fig. 2 these pixels have been replaced through interpolation in order to exclude all zero-order photons.

The local efficiency is known to depend on local plating height, line-to-space ratio, and roughness of the zone plate structure.^{10,11} For further characterization of the zone plate the plating heights of MZPs A and B were mapped in a profilometer in order to calculate¹⁰ the expected efficiency profile under the assumption of perfect line-to-space ratio and no zone edge roughness. Figure 3 shows these expected efficiency profiles together with the corresponding measured radial average efficiency of MZPs A and B. The gray-shaded regions represent estimated uncertainties in the local efficiency. Clearly, the measured local efficiency is less than the calculated one. The difference increases with radius, which indicates that the nonperfect line-to-space ratio and zone edge roughness has an increasingly impairing effect on the local efficiency as the zone width decreases towards the outer zones. Hence, it is important to improve the fabrication of MZP with respect to the line-to-space ratio and the zone

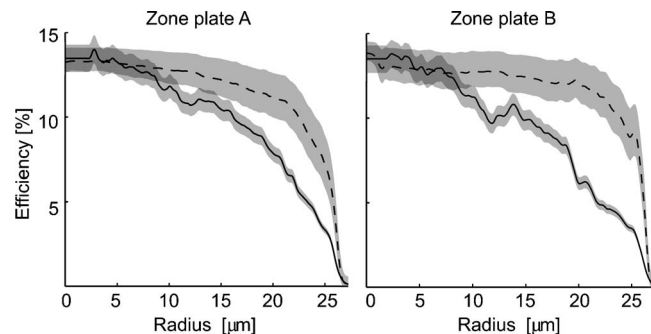


FIG. 3. Radial average efficiency profiles (continuous lines) of micro-zone plates A and B compared with calculated profiles (dashed lines) based on the plating height profile and the assumption of perfect line-to-space ratio and no roughness. Shaded areas represent error estimates.

edge roughness, especially for the outermost zones. The importance of a more uniform plating of the MZP is also indicated by the calculated efficiency profiles in Fig. 3. Increased local efficiency, especially of the outer zones, would improve the total efficiency and also the imaging properties of the MZP.

In summary, we have developed an in-house laboratory-scale laser-plasma-based method for accurate measurements of the local and absolute efficiency of MZPs. Moreover, we have shown that local efficiency maps together with radial average efficiency profiles are applicable tools, providing information about the zone plate grating pattern imperfections and their effect on efficiency. Thus, the method enables rapid feedback to the MZP fabrication process which is important for future development of improved zone plates.

The authors gratefully acknowledge the financial support of the Swedish Science Research Council. They would also like to thank Magnus Lindblom for sharing his knowledge and experience in zone plate fabrication.

¹ X-Ray Microscopy, edited by S. Aoki, Y. Kagoshima, and Y. Suzuki (The Institute of Pure and Applied Physics, Tokyo, Japan, 2006).

² D. T. Attwood, *Soft X-Rays and Extreme Ultraviolet Radiation* (Cambridge University Press, Cambridge, 1999).

³ A. Holmberg, S. Rehbein, and H. M. Hertz, *Microelectron. Eng.* **73–74**, 639 (2004).

⁴ M. Peuker, *Appl. Phys. Lett.* **78**, 2208 (2001).

⁵ M. Peuker, G. Schneider, and D. Weiss, *Proc. SPIE* **3449**, 118 (1998).

⁶ E. Ahlgqvist, Diploma thesis, Biomedical and X-Ray Physics, Royal Institute of Technology, Stockholm, 2004.

⁷ M. Peuker, *Elektronenstrahlolithographie und Nanostrukturübertragung zur Herstellung von Hochauflösenden Diffraktiven Röntgenoptiken aus Nickel* (Cuvillier Verlag, Göttingen, 2000).

⁸ P. A. C. Jansson, U. Vogt, and H. M. Hertz, *Rev. Sci. Instrum.* **76**, 43503 (2005).

⁹ T. Wilhein, D. Hambach, B. Niemann, M. Berglund, L. Rymell, and H. M. Hertz, *Appl. Phys. Lett.* **71**, 190 (1997).

¹⁰ H. W. Schnopper, L. P. Van Speybroeck, J. P. Devaille, A. Epstein, E. Kallne, R. Z. Bachrach, J. Dijkstra, and L. Lantward, *Appl. Opt.* **16**, 1088 (1977).

¹¹ A. N. Kurokhtin and A. V. Popov, *J. Opt. Soc. Am. A* **19**, 315 (2002).